Nuclear Engineering and Technology 50 (2018) 849–853

Contents lists available at ScienceDirect

Nuclear Engineering and Technology

journal homepage: www.elsevier.com/locate/net

Original Article

Semiempirical model for wet scrubbing of bubble rising in liquid pool of sodium-cooled fast reactor

Arjun Pradeep, Anil Kumar Sharma*

Indira Gandhi Centre for Atomic Research, HBNI, Kalpakkam, Tamil Nadu, India, 603102

ARTICLE INFO

Article history:
Received 10 November 2017
Received in revised form
21 February 2018
Accepted 2 April 2018
Available online 7 April 2018

Keywords:
Aerosol
Bubble
Mass Transfer
Sodium-cooled Fast Reactor Safety
Wet Scrubbing

ABSTRACT

Mechanistic calculations for wet scrubbing of aerosol/vapor from gas bubble rising in liquid pool are essential to safety of sodium-cooled fast reactor. Hence, scrubbing of volatile fission product from mixed gas bubble rising in sodium pool is presented in this study. To understand this phenomenon, a theoretical model has been setup based on classical theories of aerosol/vapor removal from bubble rising through liquid pools. The model simulates pool scrubbing of sodium iodide aerosol and cesium vapor from a rising mixed gas bubble containing xenon as the inert species. The scrubbing of aerosol and vapor are modeled based on deposition mechanisms and Fick's law of diffusion, respectively. Studies were performed to determine the effect of various key parameters on wet scrubbing. It is observed that for higher vapor diffusion coefficient in gas bubble, the scrubbing efficiency is higher. For aerosols, the cut-off size above which the scrubbing efficiency becomes significant was also determined. The study evaluates the retention capability of liquid sodium used in sodium-cooled fast reactor for its safe operation.

1. Introduction

Wet scrubbing has been used in a variety of applications to remove air pollutants and in particular for removing radioactive aerosols. Sodium-cooled fast reactors (SFRs) find several applications related to wet scrubbing phenomenon in liquid pools. The key areas in SFR, where the study finds applications are source term estimation, cover gas purification, and air cleaning systems. In the postulated accident of fuel pin failure in SFR, fission products get released from the failed pin to the primary cooling system. Among these released fission products, gaseous (xenon and krypton) and volatile fission product (VFP) gets transported to the cover gas region and further to the environment in certain cases. Therefore, the transport behavior of VFPs is very important for the assessment of radioactive consequence following fuel pin failure. When inert gases are released with volatiles into the coolant as bubbles as shown in Fig. 1, the retention of volatiles in sodium is affected by the bubble dynamics and mass transfer from the rising bubbles.

Several experimental and few theoretical studies were carried out to evaluate the cover gas source term due to VFPs (iodine, cesium) bubble transport phenomena in sodium pool. Experiments carried out till date evaluated the aerosol scrubbing efficiency for iodine during the rise of mixed gas bubble through sodium in the range from 0 to 100% [1–4], depending on the experimental conditions. The conditions considered were pool temperatures in the range of 378 K–873 K, pool depths in the range of 0.01 m–3 m, initial iodine masses in the range of 0.6 mg–2697 mg, and initial bubble diameters in the range from 7.5 mm to 120 mm. The inert gases studied were nitrogen, xenon, and krypton. Few theoretical models were also developed to evaluate the fraction of sodium iodide aerosols and cesium vapors retained by sodium pool during bubble transport [4–7]. The theoretical models developed till now were mainly for aerosol scrubbing, of which some evaluated deposition coefficients for spherical bubble shape [4,5]. The model for vapor scrubbing evaluated the efficiency based on fitted equations valid for spherical diffusion at long time scales $\left(\text{Fourier number}, Fo = \frac{D_{vi}t}{R^2} > 0.5\right)$ [6]. However, bubble rise phenomenon is characterized by shape changes and the rise time can be below the criteria for long time scale.

In this study, a simple wet scrubbing model has been developed, which evaluates the aerosol/vapor mass transfer from rising gas bubble in liquid pools typical of SFR. This theoretical model includes the application of classical theories of mass transfer, developed for a case of isolated bubble rising through liquid. The present model evaluates the deposition coefficients of aerosol scrubbing for

* *Corresponding author.*
E-mail address: aksharma@igcar.gov.in (A.K. Sharma).

https://doi.org/10.1016/j.net.2018.04.003

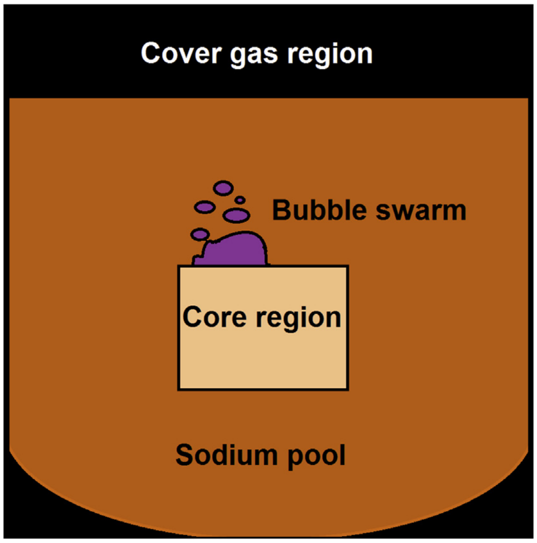

Fig. 1. Pool scrubbing during VFP bubble transport.
VFP, volatile fission product.

ellipsoidal bubble shape and analytically solves the Fick's diffusion equation to obtain the vapor scrubbing efficiency valid for all the bubble rise times typical to SFR pool. The study also provides details of parametric studies performed to determine the effect of various key parameters on pool scrubbing.

2. Model description

The wet scrubbing model comprises of modules for evaluation of bubble dynamics and mass transport of aerosol/vapor. The bubble dynamics module evaluates the bubble diameter, terminal velocity, and shape based on correlations available in literature. The mass transport module evaluates the aerosol/vapor scrubbing for bubble rise through liquid pool. The description of the wet scrubbing model is divided into the following sections.

2.1. Assumptions

In SFR, the primary system operates near atmospheric pressure. Therefore, pressure above the pool is assumed to be atmospheric in the present model. The assumption of initial bubble size as maximum stable bubble diameter is limited by hydrodynamic instability during bubble rise. The scrubbing processes considered for aerosol submodule are diffusion, sedimentation, and inertial impaction. The scrubbing of VFPs via vapor-phase condensation is not considered as it may augment/suppress the efficiency based on magnitude of evaporative flux at the gas–liquid interface. Hence, the present model assumes instantaneous thermal equilibrium between gas and liquid phases at the bubble entry point. The scrubbing process considered for vapor submodule is the diffusion of vapor to the bubble surface followed by instantaneous dissolution/reaction with liquid sodium at the gas–liquid interface and removal into sodium by its flow. The assumption is based on high solubility of cesium in sodium and significant reaction rate of iodine vapor with sodium at the bubble boundary.

2.2. Bubble dynamics module

The bubble dynamic parameters are evaluated based on the correlations available in literature. Mass transfer from the rising bubble depends on bubble diameter and terminal velocity. The maximum stable bubble diameter was evaluated from the Levich [8] correlation. The variation of bubble terminal velocity with diameter is determined from the parameterization equation developed by Park et al. [9].

$$d_b = \frac{3.6\sigma_l}{u_T^2\left(\rho_g\rho_l^2\right)^{1/3}} \tag{1}$$

$$u_T = \frac{1}{\sqrt{\frac{144\mu_l^2}{g^2\rho_l^2 d_b^4} + \frac{\mu_l^{4/3}}{0.14425^2 g^{5/3}\rho_l^{4/3} d_b^3} + \frac{1}{\frac{2.14\sigma_l}{\rho_l d_b} + 0.505 g d_b}}} \tag{2}$$

where, d_b is the bubble diameter, u_T is the terminal velocity of bubble, σ_l is the liquid surface tension, ρ_g and ρ_l are the gas and liquid densities respectively, μ_l is the dynamic viscosity of liquid, and g is the acceleration due to gravity. The bubble dynamics in terms of shape and rise velocity is characterized by nondimensional numbers, such as Morton number $\left(M = \frac{g\mu_l^4}{\sigma_l^3\rho_l}\right)$, Eötvös number $\left(Eo = \frac{\rho_l g d_b^2}{\sigma_l}\right)$, Reynolds number $Re = \frac{u_T\rho_l d_b}{\mu_l}$, and Tadaki number $(Ta = Re{\cdot}M^{0.23})$.

2.3. Mass transfer module

The mass transfer module comprises of submodules for aerosol and vapor scrubbing by liquid pools during bubble rise. The module is classified into the following sections.

2.3.1. Aerosol scrubbing in liquid pool

At higher pool temperatures, reaction between sodium vapor and iodine is significant and dominant, resulting in production of NaI aerosols at the reaction front formed in the inside of a bubble. The aerosol scrubbing efficiency of liquid pool for mixed gas bubble was obtained from aerosol removal models [6,7,10]. The deposition mechanisms considered in the present model are diffusion, sedimentation, and inertial impaction. Diffusion is due to Brownian motion and random nature of gas molecule collision. Sedimentation is due to gravitational settling, and inertial impaction occurs when molecules cannot follow the streamlines of flow. The amount deposited was calculated for a range of particle size (d_p). The deposition fractions are evaluated from the terminal velocity and bubble diameter predicted by the bubble dynamic module.

$$SE_a(\%) = \left[1 - \frac{C_a}{C_{a0}}\right] \times 100 = \left[1 - exp\left(-h^*\left(\alpha_{diff} + \alpha_{sed} + \alpha_{iner}\right)\right)\right] \times 100 \tag{3}$$

where, SE_a is the aerosol scrubbing efficiency, C_{a0} and C_a are the initial and final aerosol concentrations in the bubble, respectively, h is the pool depth, α_{diff}, α_{sed}, and α_{iner} are the deposition coefficients for diffusion, sedimentation, and inertial impaction [6,7,10], respectively.

2.3.2. Vapor scrubbing by liquid pool

Transport of VFPs (Cs, I) can also take place in vapor form, rather than as aerosol during liquid pool scrubbing. The mass transport of volatile species from a bubble into pool can be described by Fick's law, if it is assumed that the vapor reacts/dissolves instantaneously at the gas–liquid interface and is removed into the liquid pool due to sodium flow. Cesium vapor reaching the gas–liquid interface dissolves in sodium pool because of its high solubility. Iodine vapor reacts with liquid sodium instantaneously at the gas–liquid interface, and the product NaI is removed into the sodium [11]. At lower pool temperatures, sodium vapor pressure is relatively low as compared to iodine and only minimal reaction takes place between sodium vapor and iodine. Therefore, the diffusive loss of iodine to the bubble surface dominates during the rise period. The model for vapor scrubbing solves the Fick's second law of diffusion in spherical geometry starting with uniform concentration inside and zero boundary condition [6,12].

$$\frac{c_v - c_{v0}}{c_{vs} - c_{v0}} = 1 + 2\sum_{n=1}^{\infty}(-1)^n exp\left(\frac{-D_{vi}n^2\pi^2 t}{R^2}\right), \quad r = 0, \quad n = 1, 2, 3, \ldots \tag{4}$$

$$\frac{c_v - c_{v0}}{c_{vs} - c_{v0}} = 1 + \frac{2R}{\pi r}\sum_{n=1}^{\infty}\frac{(-1)^n}{n} sin\left(\frac{n\pi r}{R}\right) exp\left(\frac{-D_{vi}n^2\pi^2 t}{R^2}\right), \quad r \neq 0, n = 1, 2, 3, \ldots \tag{5}$$

$$SE_v(\%) = \left[1 - \frac{6}{\pi^2}\sum_{n=1}^{\infty}\frac{1}{n^2} exp\left(\frac{-D_{vi}n^2\pi^2 t}{R^2}\right)\right] \times 100 \tag{6}$$

where, SE_v is the vapor scrubbing efficiency, C_{v0}, C_v, and C_{vs} are the initial, final, and surface vapor concentrations of the bubble, respectively, R is the radius of the bubble, t is the time of bubble rise, r is the radial coordinate, and D_{vi} is the vapor diffusion coefficient in inert gas. The diffusion coefficient of vapor in inert gas was estimated from the Chapman–Enskog theory [12].

3. Validation

Validation has been carried out for the aerosol scrubbing submodule of the wet scrubbing model. The iodine bubble experiment [1] studied the scrubbing efficiency of sodium pool for nitrogen–iodine mixture gas bubble rising in sodium pool. The conditions considered for the experiment were pool temperatures of 533 K–811 K, pool depths of 1.8 and 3 m, initial iodine concentrations of 10, 50, and 100%, and initial bubble volume of 39 ml. The validation of aerosol scrubbing submodule of wet scrubbing model has been carried out using experimental results at high pool temperatures. At high temperatures, the iodine–sodium vapor reaction dominates as compared to the diffusion transport of iodine vapor to the bubble surface during the rise period. The experimental pool scrubbing efficiency at 811 K for pool depths of 1.8 and 3 m were observed to be more close to scrubbing efficiency predicted by the present model for aerodynamic particle diameter $(d_a = d_p(\rho_p/\rho_w)^{1/2})$ of 5.7 micron (particle diameter, d_p of 3 micron) as shown in Fig. 2.

Validation of vapor scrubbing submodule has been carried out with theoretically estimated values for xenon–cesium mixture gas bubble available in literature. Umbel [6] studied the scrubbing efficiency of sodium for xenon–cesium mixture gas bubble rising in the pool. The conditions considered for the evaluation were pool temperature and depth of 783 K and 4.47 m, respectively. Umbel used fitted equations valid for spherical diffusion at long time scales (Fo > 0.5) and evaluated the efficiencies as 99% and 99.99% at pool rise times of 3 seconds and 12 seconds, respectively. Fig. 3 shows that the efficiencies predicted by present model are lower than the values of Umbel by 11% and 0.07%. The deviation at 3 seconds in Fig. 3 arises from the longer time scale assumption in Umbel's model.

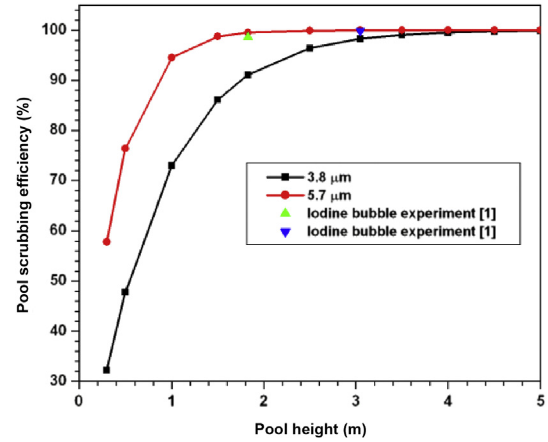

Fig. 2. Validation of aerosol submodule of wet scrubbing model.

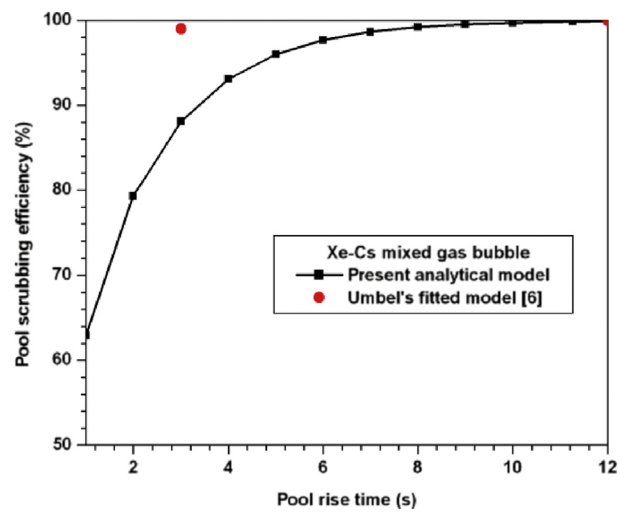

Fig. 3. Validation of vapor submodule of wet scrubbing model.

4. Results and discussion

The bubble dynamic module has been used to evaluate the variation of bubble terminal velocity with diameter and is shown in Fig. 4 for a rise height of 1 m. The terminal velocity decreases as bubble diameter increases in the range of 1–10 mm due to transition of bubble shape from spherical to ellipsoidal, after which it increases as depicted in Fig. 4. The diameters and corresponding shapes of bubble for the three *gas–liquid* systems are also given in Table 1. The results show that for all the three systems studied, the shape is ellipsoidal/spherical cap for the bubble diameters above 10 mm.

The model has been used to evaluate the bubble dynamics of xenon bubble rising in sodium pool at 800 K. The gas bubble temperature is considered to be same as the pool temperature. The rise height considered for bubble rise is 4.47 m. At temperature of 800 K, the bubble diameter is 28.9 mm, and the terminal velocity is 39.7 cm/s, which corresponds to a rise time of 11.26 seconds. The transport properties for liquid sodium and xenon gas were evaluated as function of temperature [13,14]. The nondimensional numbers considered for bubble rise are $M = 8.3 \times 10^{-15}$, $Re = 41{,}930.1$, $Eo = 43.7$, and $Ta = 24.2$. The bubble diameter increases with increase in temperature upto 800 K and further decreases based on the balance of density and surface tension forces

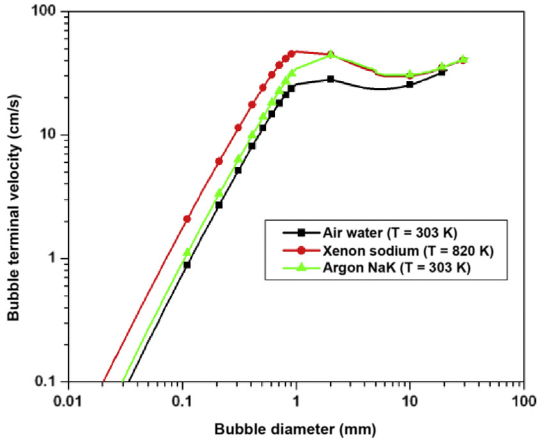

Fig. 4. Bubble terminal velocity as a function of bubble diameter.

Table 1
Bubble diameters as a function of shape.

Gas–liquid system	Spherical to ellipsoid transition diameter (mm)	Ellipsoid to spherical cap transition diameter (mm)	Maximum stable bubble diameter (mm)
Air–water	5.6	17.1	21.2
Xenon–sodium	9	27.6	30.2
Argon–NaK	9.4	29	32.9

as per Levich correlation [8]. The surface tension, liquid density, and gas density decrease with increase in temperatures of liquid and gas. The same trend is observed for the variation of bubble terminal velocity with temperature as is the case for bubble diameter. The predicted variations in bubble diameter and terminal velocity w.r.t. temperature are within 3.5 % and 1.3%. Hence, these parameters are not sensitive to sodium pool temperature.

Based on the model that evaluated bubble dynamics of xenon bubble rising in sodium pool at 800 K, the scrubbing efficiency of liquid pool for NaI aerosols contained in xenon bubble has been evaluated. Fig. 5 depicts the total scrubbing efficiency of NaI aerosols contained in xenon bubble rising through sodium pool as a function of aerodynamic particle size, which can be obtained by adding the individual contributions due to sedimentation, diffusion, and inertial impaction deposition mechanisms. It can be seen from Fig. 5, the inertial impaction mechanism accounts for majority of the overall scrubbing efficiency in the larger size range and the diffusion mechanism accounts for majority of the overall scrubbing efficiency in the smaller size range. As seen from Fig. 5, for aerodynamic particle sizes less than one micron, the scrubbing efficiency is small and is mainly governed by diffusional deposition, whereas for particles greater than one micron, the scrubbing efficiency is significant. Fig. 6, shows the overall scrubbing efficiency as a function of pool height for various aerodynamic particle sizes. It can be seen that for aerodynamic particle sizes greater than 7.6 micron for NaI aerosols, complete removal of aerosols takes place within 1 m of rise height in a sodium pool at 800 K and inertial impaction mechanism accounts for the majority of the overall scrubbing efficiency.

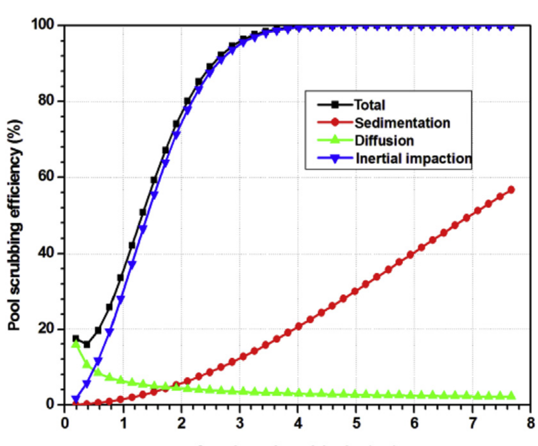

Fig. 5. Pool scrubbing efficiency for NaI as a function of aerodynamic particle diameter.

Based on the model that evaluated bubble dynamics of xenon bubble rising in sodium pool at 800 K, the scrubbing efficiency of liquid pool for Cs vapor contained in xenon bubble has been evaluated. A diffusion coefficient of 2.3×10^{-5} m^2/s is estimated for the

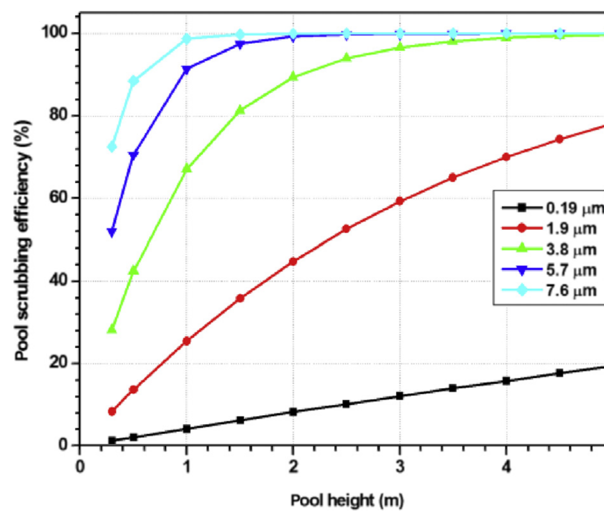

Fig. 6. Pool scrubbing efficiency for NaI aerosol as a function of pool height for various aerodynamic particle diameters.

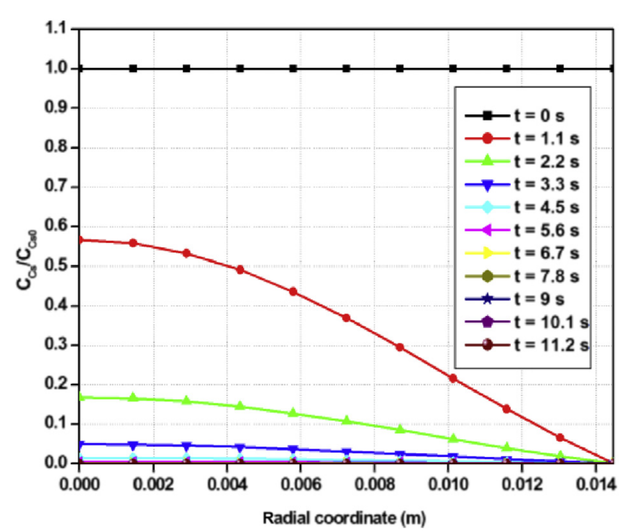

Fig. 7. Pool scrubbing model for Cs vapor diffusion from a Xe–Cs mixed gas bubble into liquid sodium.

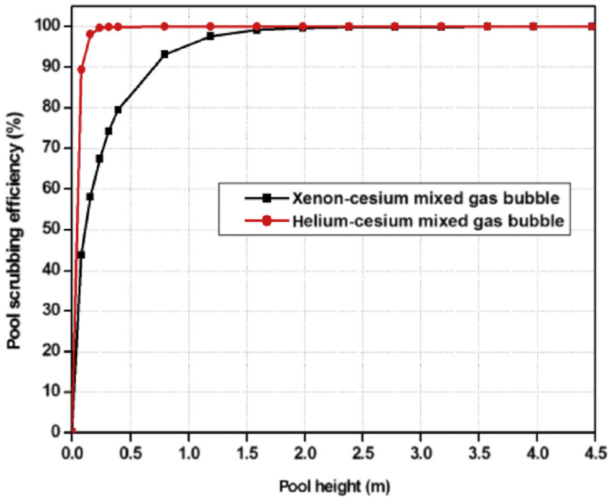

Fig. 8. Pool scrubbing efficiency for Cs vapor diffusion as a function of pool height.

Table 2
Effect of inert gas component on scrubbing efficiency.

Inert gas component	Rise time (s)	Diffusion coefficient (m^2/s)	Scrubbing efficiency (%)
Xe	3	2.3×10^{-5}	97.74
He	3	1.8×10^{-4}	99.99

diffusion of cesium in xenon bubble at 800 K. The vapor scrubbing efficiency is 99.99% for bubble rising through a typical SFR pool of 4.47 m. The variation of cesium concentration along the radial coordinate of the bubble at different bubble rise times is shown in Fig. 7. However, the rise time for bubble is substantially less considering the initial flow velocity, expansion of bubble in the channel, and swarm effect. A rise time of 3 s results in a scrubbing efficiency of 97.74 %. These calculations were based on cesium vapor diffusion in xenon gas. The bubble is also likely to contain krypton and helium. The diffusion coefficient for cesium diffusion in helium is nearly an order of magnitude larger, and the scrubbing efficiency is therefore larger as shown in Fig. 8 and Table 2. This suggests that the amount of cesium vapor bypassing the pool via bubble transport is smaller for inert gases with lower molecular weight.

The precise contribution of this model is that inertial impaction and diffusion are responsible for most of the liquid pool scrubbing of very large and very small aerosol particles, respectively. Results of the analysis suggest that essentially all of the large particles greater than four microns are removed during bubble rise through a 1 m deep pool. Vapor scrubbing efficiency is higher for lower molecular weight of inert gas due to the higher vapor diffusion coefficient.

5. Conclusion

A pool scrubbing model has been setup to evaluate the scrubbing efficiency of aerosol/vapor from rising gas bubbles in liquid pools of SFR. The model comprises of modules for evaluation of bubble dynamics and mass transport of aerosol/vapor. The model considers aerosol (NaI) capture by Brownian diffusion, inertial deposition, and gravitational sedimentation. The model simulates the scrubbing of volatile vapors (Cs, I) based on molecular diffusion in spherical geometry starting with uniform concentration inside and zero boundary condition. The present model has been validated for the aerosol and vapor submodules based on experimental and theoretical results available in literature. It is observed that for higher vapor diffusion coefficient in gas bubble, the vapor scrubbing efficiency is higher. For aerosols, the cut-off size above which the scrubbing efficiency becomes significant was also determined. Both vapor and aerosol scrubbing efficiency increases with increase in height of the pool/rise time. The pool scrubbing model is useful for source term evaluation and estimating the scrubbing efficiency of liquid pools in SFRs.

Conflicts of interest

All authors have no conflicts of interest to declare.

References

[1] W.P. Kunkel, Fission-product Retention in Sodium: a Summary of Analytical and Experimental Studies at Atomics International, NAA-SR-11766, Atomics International, Canoga Park, Calif, 1966.
[2] Quarterly Technical Progress Report, Nuclear Safety, Characterization of Sodium Fires and Fast Reactor Fission Products, AI-ERDA-13172, Atomics International, January-March 1976.
[3] S. Miyahara, N. Sagawa, K. Shimoyama, Iodine mass transfer from xenon-iodine mixed gas bubble to liquid sodium pool, (I) experiment, J. Nucl. Sci. Technol. 33 (1996) 128–133.
[4] S. Miyahara, N. Sagawa, K. Shimoyama, Experimental and Analytical Studies of Iodine Mass Transfer from Xenon-Iodine Mixed Gas Bubble to Liquid Sodium Pool, Technical Committee Meeting on Evaluation of Radioactive Materials Release and Sodium Fires in Fast Reactor, IWGFR/92, O-arai, Japan, 1996.
[5] S. Miyahara, N. Sagawa, Iodine mass transfer from xenon-iodine mixed gas bubble to liquid sodium pool, (II) Development of analytical model, J. Nucl. Sci. Technol. 33 (1996) 220–228.
[6] M. Umbel, Containment Source Terms for Sodium-Cooled Fast Reactor Accidents, Master of Science Thesis, The Ohio State University, 2011, https://etd.ohiolink.edu/!etd.send_file?accession=osu1306506275&disposition=inline.
[7] M. Bucknor, M. Farmer, D. Grabaskas, An Assessment of Fission Product Scrubbing in Sodium Pools Following a Core Damage Event in a Sodium Cooled Fast Reactor, Argonne National Laboratory (ANL), 2017.
[8] V.G. Levich, Physiochemical Hydrodynamics, Prentice Hall, Englewood Cliffs, New Jersey, 1962.
[9] S.H. Park, C. Park, J. Lee, B. Lee, A Simple Parameterization for the Rising Velocity of Bubbles in a Liquid Pool, Nucl. Eng. Technol. 49 (2017) 692–699.
[10] D.A. Powers, J.L. Sprung, A Simplified Model of Aerosol Scrubbing by a Water Pool Overlying Core Debris Interacting with Concrete, NUREG/CR-5901, 1992.
[11] S. Miyahara, K. Shimoyama, Transport phenomena of iodine and noble gas mixed bubbles through liquid sodium, in: Liquid Metal Systems, 1995, pp. 27–33.
[12] J.R. Welty, C.E. Wicks, G. Rorrer, R.E. Wilson, Fundamentals of Momentum, Heat and Mass Transfer, John Wiley and Sons, 2009.
[13] J.K. Fink, L. Leibwitz, Thermodynamic and Transport Properties of Sodium Liquid and Vapor, ANL/RE-95/2IL, Argonne National Lab., United States, 1995.
[14] J. Kestin, S.T. Ro, W.A. Wakeham, Viscosity of the noble gas in the temperature range 25 – 700 °C, J. Chem. Phys. 56 (1972) 4119–4124.